HHS Public Access

Author manuscript

Mol Cancer Ther. Author manuscript; available in PMC 2021 August 27.

Published in final edited form as:

Mol Cancer Ther. 2013 November ; 12(11): 2389–2399. doi:10.1158/1535-7163.MCT-13-0132.

Paclitaxel-Hyaluronic Nano-Conjugates Prolong Overall Survival in a Preclinical Brain Metastases of Breast Cancer Model

Rajendar K. Mittapalli[1], **Xinli Liu**[1], **Chris E. Adkins**[1], **Mohamed I. Nounou**[1], **Kaci A. Bohn**[1], **Tori B. Terrell**[1], **Hussaini S. Qhattal**[1], **Werner J. Geldenhuys**[2], **Diane Palmieri**[3], **Patricia S. Steeg**[3], **Quentin R. Smith**[1], **Paul R. Lockman**[1,*]

[1]Department of Pharmaceutical Sciences, School of Pharmacy, Texas Tech University Health Sciences Center, Amarillo, TX 79106.

[2]Department of Pharmaceutical Sciences, Northeast Ohio Medical University, College of Pharmacy, Rootstown, OH, 44272.

[3]Women's Cancers Section, Laboratory of Molecular Pharmacology, Center for Cancer Research, National Cancer Institute, Bethesda, MD

Abstract

Brain (CNS) metastases pose a life-threatening problem for women with advanced metastatic breast cancer. It has recently been shown that the vasculature within preclinical brain metastasis model markedly restricts paclitaxel delivery in ~90% of CNS lesions. Therefore to improve efficacy, we have developed ultra-small hyaluronic acid (HA) paclitaxel nano-conjugates (~5kDa) that can passively diffuse across the leaky blood-tumor barrier and then be taken up into cancer cells (MDA-MB-231Br) via CD44 receptor mediated endocytocis. Utilizing CD44 receptor-mediated endocytosis as an uptake mechanism allowed paclitaxel to bypass p-glycoprotein mediated efflux on the surface of the cancer cells. *In vitro* cytoxicity of the conjugate and free paclitaxel were similar in that they 1) both caused cell cycle arrest in the G_2/M phase 2) demonstrated similar degrees of apoptosis induction (cleaved caspase) and 3) had similar IC_{50} values when compared to paclitaxel in MTT assay. A preclinical model of brain metastases of breast cancer using intracardiac injections of Luc-2 transfected MDA-MB-231Br cells was used to evaluate *in vivo* efficacy of the nanoconjugate. The animals administered with HA-paclitaxel nanoconjugate had significantly longer overall survival compared to the control, and paclitaxel treated group ($p<0.05$). This study suggests that the small molecular weight (MW) HA-paclitaxel nano-conjugates can improve standard chemotherapeutic drug efficacy in a preclinical model of brain metastases of breast cancer.

Introduction:

The incidence of brain metastases is increasing and represents an emerging cause of mortality in women with metastatic breast cancer (1, 2). Current therapeutic options

*Corresponding Author: Paul R. Lockman, BSN, Ph.D., Department of Pharmaceutical Sciences, Texas Tech University, Health Sciences Center, 1406 S. Coulter Dr., Amarillo, Texas, 79106-1712, 806-356-4750 ext 227, paul.lockman@ttuhsc.edu.

The authors declare no conflict with this work.

involving chemotherapy, surgery, and or radiation have generally had limited efficacy in eradicating metastatic lesions (3, 4). A major reason for the failure of chemotherapy is that the normal blood-brain barrier (BBB) and the resultant blood-tumor barrier (BTB) limit drug distribution to sub-therapeutic levels (5, 6). To overcome poor drug distribution to metastatic lesions, we report here the formulation of small HA-paclitaxel nanoconjugate that uses a passive targeting mechanism to increase drug distribution into the tumor interstitial space and an active targeting mechanism to improve the intracellular uptake of paclitaxel into the metastatic cancer cells.

The intact BBB is the vascular interface between the blood and brain, and protects the central nervous system (CNS) from harmful toxins, by acting as a physical, enzymatic, and transport barrier. This barrier functionally limits brain penetration of many small and large therapeutic molecules (7). It has been suggested that >98% of CNS drugs fail to go into clinical trials due to poor brain penetration (8). In contrast, the BTB (the vasculature within and potentially immediately adjacent to a brain metastasis) is generally more permeable than the BBB. In our previous work (5), it was observed that BTB in metastatic lesions is permeable enough to allow initial paracellular diffusion of a ~ 4 kDa dextran into brain metastases.

To take advantage of the increased paracellular permeability, we have conjugated paclitaxel to an ~3–5 kDa polymerized hyaluronic acid (HA), which mimics the size of the dextrans which were able to penetrate the metastatic lesions (5). We hypothesize that this polymer conjugate of paclitaxel will increase drug concentrations in the metastatic lesions by 1) allowing paracellular diffusion of the paclitaxel-conjugate from blood through the BTB openings to the tumor interstitial space and 2) paclitaxel will no longer be subject to various BBB and BTB efflux transporters [e.g., p-glycoprotein (P-gp), breast cancer resistance protein (BCRP)] that normally limit paclitaxel brain and tumor distribution (9, 10).

We hypothesize that, once the paclitaxel conjugate is in the tumor interstitial space, the ultra-small nano-conjugate (~2–3 nm) actively targets the metastatic cancer cell by CD44 receptor-mediated endocytosis (11, 12). CD44 (clusters of differentiation 44) is a cell surface receptor that binds to HA and undergoes receptor-mediated endocytosis to internalize HA(13). CD44 has been shown to be overexpressed in many tumors including breast and metastatic brain (14–18). The polymeric HA exhibits a number of properties as an ideal drug carrier system. HA is water soluble, biocompatible, and as a polysaccharide, it has multiple different functional groups for potential chemical conjugation (11, 19–21) with numerous chemotherapeutic agents such as doxorubicin and paclitaxel (22–25). Consequently, we propose the use of HA to target CD44 mediated endocytosis as a novel BTB transit pathway (Fig. 1).

In this report, we demonstrate that the synthesized HA-paclitaxel nanoparticulate conjugate is 1) able to bypass P-gp efflux transporters at the BTB and the 231Br metastatic cancer cells, 2) internalized into tumor cells via CD44 receptor-mediated endocytosis, 3) causing G_2/M cell cycle arrest and cytotoxicity at levels similar to free paclitaxel, and 4) significantly increasing the median survival time in a preclinical model of triple negative brain metastasis of breast cancer.

Materials and Methods:

Chemicals:

Ultra low molecular weight HA was purchased from R&D systems (~ 4–5 kDa) (Minneapolis, MN, USA). ^{14}C-paclitaxel (specific activity 75.6 mCi/mmole) was purchased from Moravek Biochemicals Inc. (Brea, CA, USA). Paclitaxel and Texas Red hydrazide were purchased from Molecular Probes Invitrogen (Eugene, Oregon, USA). Cyclosporin A was purchased from Toronto Research Chemicals Inc. (Toronto, Canada). 2-chloro-1-methyl pyridinium iodide, triethylamine, 4-dimethyl aminopyridine (DMAP), dicyclohexyl carbodiimide (DCC), poly (ethylene glycol) dimethyl ether (dmPEG) (MW: 2000 Da), Cremophor EL, and anhydrous dimethyl sulfoxide (DMSO) were purchased from Sigma Aldrich Inc. (St.Louis, MO, USA). All other chemicals used were of analytical grade and used as supplied.

Cell culture:

Human breast cancer cells MCF-7 and P-gp over expressing, adriamycin-resistant, MCF-7/AdrR cells were kindly donated by Dr. US Rao, Texas Tech University Health Sciences Center, Amarillo TX (26, 27). The cells were maintained in Dulbecco's modified Eagle's medium, supplemented with 10% (v/v) fetal bovine serum and antibiotics (penicillin, 100 U/mL; and streptomycin, 100 μg/mL). Luc-2 transfected human MDA-MB-231Br cells were kindly provided by Dr. Patricia Steeg from the National Cancer Institute (not authenticated by our laboratory). The cells were maintained in Dulbecco's modified Eagle's medium, supplemented with 10% (v/v) fetal bovine serum. Cells were grown in a 37°C humidified incubator with 5% CO_2.

Western blot:

The protein concentrations after lysis of cells were quantified using a BCA pierce assay kit (Pierce; Rockford, IL). Protein samples (20 μg per lane) were resolved by SDS-polyacrylamide gel electrophoresis and transferred to PVDF membranes. Membranes were blocked with 5% non-fat dry milk for 1 hr, after which membranes were incubated with anti-CD44 antibody at 4°C overnight. Membranes were then washed and incubated with respective HRP-conjugated secondary antibodies. Proteins were visualized using SuperSignal West Pico Chemiluminescence system (Pierce, Rockford, IL USA).

Immunocytochemistry (ICC):

Cells were grown to ~70% confluency on tissue culture treated cover slips. Cells were fixed with ice-cold acetone methanol (1:1, v/v), washed with PBS, and then incubated with 5% goat serum for 1 hr. Then the cells were incubated overnight with an anti CD44 antibody (Cell signaling technologies; Beverly, MA, USA) at a dilution of 1:200. The primary antibody was removed by repetitive washings with PBS. Afterwards, cells were incubated with nuclear stain DAPI and Alexa Fluor conjugated secondary antibodies (Molecular Probes Invitrogen, Eugene, Oregon, USA) for 1 hr. Fluorescent images were taken with an Olympus IX81 microscope (Center Valley, PA).

Conjugation of HA with paclitaxel or Texas Red:

Paclitaxel was conjugated to hyaluronic acid using a previously published method (Fig. 2) (28). Initially, a nano-complex between HA and dmPEG was formed (28). The HA polymer used was purified and desalted, where, 1g of HA (~4–5 kDa) was dissolved in 100 mL of deionized water, and dialyzed for 24 hr (MWCO: 1kDa), after which the sample was lyophilized. Then the desalted HA, and dmPEG (MW: 2000 Da) (at a molar ratio of 1:10) were dissolved in deionized water and stirred for 8 hrs and then lyophilized to give a white cotton like product. Then the HA/dmPEG was conjugated to paclitaxel using DMAP/DCC as a coupling agent. The hydroxyl groups of paclitaxel were conjugated to the carboxylic groups of HA to form an acid-cleavable ester linkage. HA/dmPEG, DCC, DMAP were added to DMSO and the resulting solution was stirred at room temperature for 1 hr. Afterwards, paclitaxel in DMSO was added to the above mixture and stirred under N_2 at 40°C for 48 hrs. The final product was transferred to a dialysis bag (MWCO: 1kDa) and dialyzed against DMSO for 24 hrs, followed by 48 hrs against water, and the resulted compound was lyophilized. The yield of conjugates was approximately 60%. Particle size of HA-paclitaxel conjugate was measured by dynamic light scattering using a Malvern Zetasizer Nano ZS90 (Malvern Inc., Westborough, MA). The size measurement was carried out at a concentration of 7.0 mg/mL of conjugate in PBS at room temperature. ^{1}H-NMR spectra of HA-paclitaxel conjugate was obtained by Bruker NMR spectrometer (Bruker, Germany) using deuterated DMSO-d6 (Fig. S1). The amount of paclitaxel conjugated to HA was determined by HPLC using a 50:50 mixture of acetonitrile and water as cosolvent. Eluted compounds were detected at 227 nm using a UV-vis detector. Free paclitaxel was used as standard to generate a standard curve and the paclitaxel conjugated to HA was determined to be 8% (w/w%). This level of conjugation was slightly smaller than previous reported (10.8%) (28).

Fluorescent conjugates of HA were also synthesized by condensation of Texas Red hydrazide to HA as previously described (29). Briefly, HA was activated with 2-chloro-1-methyl pyridinium iodide and triethylamine. Then Texas Red hydrazide (5 mg in 1 mL of DMSO) was added and the mixture was refluxed for 24 hrs, followed by 48 hr dialysis against water at 4°C, and the resulting compound was lyophilized.

Cellular uptake and Competitive inhibition studies:

For competitive inhibition studies, the MDA-MB-231Br cells were incubated in 2 mL of serum free media containing HA (0.625 μM) with HA conjugates for 90 minutes. For fluorescent microscopy studies with HA-TX Red, the cells were washed twice in PBS and fixed with ice-cold acetone: methanol (50:50). The intracellular accumulation of HA-TX Red was visualized using an Olympus IX81 stereo microscope. For ^{14}C-HA-paclitaxel studies, after incubation period the cells were washed in PBS, followed by lysis in RIPA lysis buffer. The radioactivity in cell lysates was determined using a Beckman liquid scintillation counter. To determine if the formulation bypassed P-gp efflux; P-gp over expressing cells, grown in 12-well plates, were utilized to determine the cellular uptake of ^{14}C-paclitaxel and ^{14}C-HA-paclitaxel. Cells were washed three times with PBS, then incubated with or without 10 μM cyclosporin A (a classical p-gp inhibitor) for 30 min in serum free media. Then the tracers were added and further incubated for 60 min. The

cells were washed three times with ice cold PBS, and cell lysis was accomplished using lysis buffer. The amount of tracer in cell lysates was determined using a Beckman liquid scintillation counter with appropriate correction for quench, background and efficiency. An aliquot of cell lysates was utilized to determine protein content.

Receptor mediated endocytosis of HA-paclitaxel naoconjugates in 231Br cells:

231Br cells were seeded in 12-well plates at the density of 5×10^4 cells per well and incubated for 24 hr. After checking for confluency, media was aspirated from the wells and cells were washed with PBS three times. The cells were incubated with different endocytic inhibitors [methyl-β-cylcodextrin (5 mM), chlorpromazine hydrochloride (10 μg/mL) and nystatin (25 μg/mL)], for 30 min. Then ^{14}C-HA-Paclitaxel was added to each well and incubated for 60 min. After incubation, treatment solutions were aspirated and cells were washed three times with ice-cold PBS. Then the cells were lysed with RIPA lysis buffer and an aliquot of lysate was transferred to scintillation vial containing scintillation fluid. Amount of ^{14}C-HA-Paclitaxel present in the lysate was determined by counting the *dpms* (disintegrations per minute) using scintillation counter. Uptake of ^{14}C-HA-Paclitaxel was normalized with respect to total protein content determined using Bradford Assay.

Cell cycle analysis using flow cytometry:

231Br cells were grown to ~70% confluency and treated with equimolar concentrations of either paclitaxel or HA-paclitaxel for 24 hrs. After treatment, cells were trypsinized, centrifuged, washed twice with PBS, and then fixed with 70% ice cold ethanol for 24 hrs. Fixed cells were washed twice in PBS to remove excess ethanol, after which cells were incubated at 37°C with DNA staining solution containing propidium iodide (50 μg/mL). Cells were analyzed with a FACS Scanner flow cytometer (BD Biosciences: NJ, USA).

In vitro cytotoxicity:

231Br cells were seeded at a density of 10^4 cells per well in 48 well plates. Cytotoxicity was determined by treating the cells with equimolar concentrations of either paclitaxel or HA-paclitaxel for 48 hrs. Cell viability was determined using MTT assay. 60 μl (2mg/ml) of dimethyl thiazolyl diphenyl tetrazolium salt (MTT) in 1X PBS was added to the the cells, which were incubated for an additional 4 hours at 37° C. Afterward, the media was removed and 250 μl DMSO was added to each well to dissolve the formazan crystals. The absorption was measured at 570 nm using a BioTek Instrument ELx800™ microplate reader. Each sample was prepared in triplicate and the data were reported as mean ± SEM. The percentage cell viability of each sample was determined relative to the control (untreated) cells.

In vivo efficacy of HA-paclitaxel nanoconjugates:

The anti-metastatic activity of the conjugate was determined in a preclinical model of brain metastasis of breast cancer. The 231Br breast cancer cell line was previously selected for brain tropism (BR) based upon multiple rounds of *in vivo* passage in immune compromised mice (1, 30). To develop brain metastases, immune compromised NuNu female mice were anesthetized with isofluorane (0.5–2%) and inoculated with 1.75×10^5 human 231Br/100

μL into the left cardiac ventricle in serum-free media using a stereotaxic apparatus (Stoelting: IL, USA). Tumors seeded the brain and developed lesions over ~2–6 weeks, or until neurological symptoms appeared. Three days after the tumor cell injection, animals were randomly divided into one of the three treatment groups: control, paclitaxel, or HA-paclitaxel. The animals were treated with vehicle alone or paclitaxel or HA-paclitaxel [6 mg/kg (paclitaxel equivalent), once a week, intravenously for five doses]. Paclitaxel was dissolved in a vehicle composed of a 1:1 blend of Cremophor EL (polyethoxylated castor oil) and ethanol was then diluted (7 parts of saline to 3 parts of blend) with normal saline for administration. HA-paclitaxel was dissolved in normal saline. All the formulations were prepared freshly on the day of dosing. Animals were monitored over a period of 90 days for neurologic symptoms at which point bioluminescence was performed and animals sacrificed. All animal experiments were performed in accordance with approved animal use and care protocols.

Histological confirmation (cresyl violet staining):

Brain sections were rehydrated briefly, fixed in 4% paraformaldehyde (4°C), and subsequently washed. Cresyl violet stain (0.1% cresyl violet acetate) was added to each section for 15 minutes then rinsed with distilled water and placed in ethanol of increasing concentrations (70%, 95%, and 100%) for differentiation of stain. Slides were then placed in xylene for clearing, air dried, and mounted with DPX medium.

Bioluminescence:

Accuracy of left cardiac ventricle injection was confirmed using bioluminescenct imaging at 24 hr post-injection with cells. Briefly, animals were injected with D-Luciferin (150 mg/kg, i.p.) and 10–15 minutes later were imaged utilizing a Caliper Lumina XR imager and Living Image® software (Xenogen, Alameda, CA) with a 5-minute image acquisition. After development of neurological symptoms (within 90 day window), animals were imaged for bioluminescent signal to confirm presence of tumor in brain.

Statistics:

Data in all experiments represent mean ± SEM. Experiments were analyzed using ANOVA followed by Bonferonni's multiple comparison's test. For the survival data, 24 h after intra-cardiac injection animals were verified to have BLI signal from brain and were then randomized to the three groups. A Kaplan-Meier curve was obtained and a log-rank value was determined. A significance level of $p < 0.05$ was used for all experiments. (GraphPad® Prism 5 software).

Results:

CD44-HA as a novel BTB transit pathway:

CD44 is an extensively studied adhesion molecule that binds HA found in the extracellular matrix (11). Once HA is bound to the CD44 receptor, CD44 undergoes receptor mediated endocytocis to internalize HA (13). In this study, the ability of 231Br cells to internalize the ~3–5kDa HA-paclitaxel conjugate through the CD44 receptor-mediated endocytocis pathway was investigated as a novel method to improve the uptake of paclitaxel. CD44 was

observed to have a relatively high degree of expression in 231Br cells (Fig. 3A and 3B). Further, this cellular phenotype was retained *in vivo* in brain metastatic lesions (Fig. 3C). Consequently, we hypothesized that conjugation of HA to normally impermeant molecules would permit their uptake into brain metastases.

After we observed the presence of CD44 in our model system, we conjugated HA to Texas Red, a sensitive marker of BBB and BTB permeability (5) to quantify uptake of HA polymers within the 231Br cells. Fluorescent conjugates of HA were synthesized by condensation of Texas Red hydrazide to HA (Fig. 2). The HA-TX Red conjugate accumulated in the 231Br cells over a 90 min incubation (Fig. 4A). Cellular accumulation of the HA-TX Red conjugate was inhibited by ~50% with the addition of 0.625 μM of unlabeled large molecular weight (1600kDa) HA [$p<0.05$; (-)HA (100.0 ± 34.4 %); (+)HA (48.4 ± 25.2 %)] due to competitive inhibition at the CD44 receptor (Fig. 4A; left bars).

To determine if the HA-CD44 interaction was capable of delivering therapeutically relevant concentrations of drugs into experimental brain metastases, similar studies were conducted with HA conjugated to paclitaxel. The HA/dmPEG was conjugated to paclitaxel using DMAP/DCC as a coupling agent (Fig. 2). The HA-^{14}C-paclitaxel conjugate accumulated in the metastatic cells and was inhibited by the presence of free HA (Fig. 4A; right bars) [$p<0.05$; (-)HA (100.0 ± 31.2 %); (+)HA (51.8 ± 4.2 %)] due to competitive inhibition. These data suggest HA-conjugation facilitates cellular uptake via receptor-mediated endocytosis of both Texas Red and paclitaxel.

Mechanisms of cellular internalization:

To address the mechanisms of cellular internalization of the HA-paclitaxel conjugate, we observed the uptake of HA-^{14}C-paclitaxel in 231Br cells for 60 minutes in the presence of three endocytosis inhibitors, methyl-β-cylcodextrin (5mM), chlorpromazine hydrochloride (10 μg/mL) and nystatin (25 μg/mL). In separate experiments, the inhibition of clathrin mediated endocytosis (31) with chlorpromazine hydrochloride (10 μg/mL) and the inhibition of caveolae mediated uptake with nystatin (25 μg/mL) (32) did not alter the cellular uptake of ^{14}C-HA-Paclitaxel. However, inhibition of the CD44 lipid raft pathway (33) by Methyl-β-Cyclodextrin (MβCD, 5 mM) (34) reduced the cellular uptake of ^{14}C-HA-Paclitaxel by approximately 50% compared to control (Fig. 4B, **$p<0.05$**). The data further confirms an active mechanism is present which facilitates uptake of the HA-paclitaxel conjugate into the cell.

To test whether the HA conjugates would also bypass P-gp, the uptake of ^{14}C- paclitaxel and HA-^{14}C-paclitaxel in P-gp overexpressing cells in the presence or absence of the P-gp inhibitor cyclosporine A was determined. Fig. 5 shows that ^{14}C-paclitaxel uptake in 231Br cells is significantly (~7–8 fold; $p<0.0001$) increased in the presence of cyclosporine A [(−) cyclosporin A (0.97 ± 0.45 μCi/gm); (+)cyclosporin A (6.5 ± 1.7 μCi/gm)]. Furthermore, the uptake of HA-^{14}C-paclitaxel is significantly ($p<0.05$) higher than the ^{14}C-paclitaxel control (~12 fold: 11.6 ± 2.1 μCi/gm) and is not further increased by the addition of cyclosporine A (Fig. 5). This suggests that the HA conjugate bypasses P-gp and may enhance delivery of paclitaxel in metastatic brain lesions.

HA-Paclitaxel conjugates brain metastatic cells cytotoxicity:

Paclitaxel acts by binding and stabilizing the microtubules, which ultimately results in a G_2/M arrest of the cell cycle (35, 36). To determine whether HA-paclitaxel retained the same chemotherapeutic activity as paclitaxel, a cell cycle analysis was performed for both compounds using flow cytometry. Briefly, 231Br cells were treated with equimolar paclitaxel (100 nM) concentrations of either paclitaxel or HA-paclitaxel for 24 hrs after which the cells were stained with propidium iodide and DNA content was analyzed. As shown in Fig. 6A, both paclitaxel and HA-paclitaxel caused significant ($n=3$, $p<0.05$) cell cycle arrest at the G_2/M phase (70.0 ± 12.2% and 56.0 ± 10.2% of cells respectively) as compared to control (17.0 ± 7.0%). Further, after paclitaxel and HA-paclitaxel treatment, there was a similar degree of apoptosis as evidenced by cleaved caspase-3 staining (data not shown). Paclitaxel and HA-paclitaxel had similar ($p>0.05$) *in vitro* cytotoxicity towards the 231Br breast cancer cell line with an IC_{50} of 3.3 nM for HA-paclitaxel and 4.4 nM for free paclitaxel (Fig. 6B).

In vivo efficacy of HA-paclitaxel:

In the final set of experiments, the HA-paclitaxel conjugate was evaluated for *in vivo* efficacy in a preclinical model of brain metastases of breast cancer. One day after the intra-cardiac injection of the 231Br cell lines, animals were imaged using bioluminescence to verify the presence of metastatic cells in the brain region (Fig. S2). After verification, animals were randomized to one of three groups; vehicle, intravenous paclitaxel (6 mg/kg) or intravenous HA-paclitaxel (6 mg/kg paclitaxel equivalent). Animals were treated weekly for five doses. In the animals receiving the HA-paclitaxel conjugate, overall survival was longer compared to control ($p=0.0345$, by log rank test) and paclitaxel treated groups ($p=0.0283$, by log rank test). Similarly, lesion burden in brain was significantly decreased in the HA-paclitaxel group compared with the control and paclitaxel groups ($p<0.05$) using bioluminescence imaging (Fig. 7A). The median survival time was 37, 42, and 49 days for control, paclitaxel, and HA-paclitaxel respectively (Fig. 7B). Terminal bioluminescence imaging was verified by histology in animals (representative image shown in Fig. S3).

Discussion:

Brain metastases pose a significant problem for women with advanced breast cancer. Younger age HER-2 and triple-negative status may be the greatest risk factor for CNS metastasis development (37). Triple-negative patients who develop CNS metastases have approximately one half the time between initial diagnosis and cerebral relapse (22 vs. 51 months), and a significantly decreased survival time after initial diagnosis (4 vs. 8–15 months) (37). While there has been work completed on developing new drugs to treat brain metastases of breast cancer, clinical trials of standard, novel and combinatorial chemotherapeutic regimens have been consistently disappointing. One aspect of this problem is that the brain remains, at least in part, a sanctuary site by the continued presence of some fraction of the BBB. New methods to traverse the BBB may hold widespread promise for the development of effective brain metastasis treatments and preventatives.

Herein, we present data demonstrating that the widely expressed receptor-ligand pair CD44 and HA may be engineered small enough to pass through the leaky vasculature of the BTB and still retain the ability to be taken up into cancer cells via receptor mediated endocytocis. Further, the HA-paclitaxel nanoconjugate bypasses P-gp efflux mechanism in 231Br cells and accumulates intracellularly to a greater degree than free paclitaxel. Ultimately, the HA-paclitaxel inhibits the cell cycle at G_2/M phase, induces apoptosis and induces cytotoxicity at similar concentrations of free paclitaxel. *In vivo* efficacy studies showed that the median survival of mice improved significantly with HA-paclitaxel in breast metastasis to brain tumor model.

This novel formulation facilitates paclitaxel accumulation in 231Br cells through receptor mediated endocytocis and bypasses p-gp efflux transporters present on the cell membrane. Similar to other tumor cell lines, the 231Br cell line overexpresses CD44 (38, 39) and is able to internalize a HA-drug conjugate. This type of active targeting has been used previously to increase cellular uptake of doxorubicin loaded liposomes (~20 fold) (40). However, this work is different from most prior studies, in that the other studies utilized high molecular weight HA (>75 kDa) as the drug carrier (28, 41–43). We chose to use the smaller molecular weight HA since our previous work demonstrated that in the preclinical model a ~ 4kDa dextran was able to accumulate in numerous metastatic lesions, but the 70kDa dextran had a more limited penetration (5). Importantly, the size of our formulation was observed to be in two distinct populations; one of 2–3 nm and the other at approximately 80 nm. We believe that the smaller conjugates can self-assemble into larger particles similar in structure to a lipid membrane. Based upon previous work, it is unlikely that the larger particles enter into the brain metastases. It is likely that the single molecules, as well as single molecules released from the aggregates are the active component and responsible for the effect.

One concern in using the lower molecular weight HA is the binding affinity of HA to CD44, which depends on the number of disaccharides present on the HA molecule (44). However, our data demonstrated that the ultra-low molecular weight HA polymer used in this study to conjugate to paclitaxel retained the ability to be internalized into the cell via receptor-mediated endocytocis. These data are consistent with previous studies demonstrating oligomers of HA with as low as 4 to 14 sugar residues, were still able to undergo receptormediated endocytocis (44).

Paclitaxel, has low water solubility (13) and has limited brain distribution primarily due to the BBB efflux transporter, P-gp (10, 45, 46). Several strategies have been employed to circumvent P-gp at BBB, including chemical modification, (47) encapsulating in nanoparticles (48) and conjugating to peptide vectors (49–52). Our data suggest that HA-paclitaxel bypasses P-gp, and the cellular uptake of the conjugate is ~10 fold greater than that of free paclitaxel. These data are in agreement with prior reports, where the conjugation of drugs such as doxorubicin and paclitaxel to peptides resulted in decreased affinity of the compound for P-gp at BBB (52, 53). For example, ANG1005, a conjugate of angiopep-2 with three molecules of paclitaxel showed ~5 fold increase in brain uptake than free paclitaxel in P-gp knockout mice (54, 55). Similarly, when doxorubicin was conjugated to a peptide (penetratin), the brain parenchymal accumulation was increased ~4–5 times greater than doxorubicin (56).

Paclitaxel stabilizes microtubules and interferes with the G_2 and M phases of the cell cycle (35, 36, 57). Our data demonstrate that HA-paclitaxel causes a similar arrest at the G_2/M phase of cell cycle. Further, the HA-paclitaxel conjugate had a slightly lower IC_{50} in the 231Br cells than that of free paclitaxel. From These data, we speculate that HA-paclitaxel retains similar cytotoxicity mechanisms as that of paclitaxel. This may be possible since the HA-conjugate is designed to be cleaved by cytosolic hyaluronase enzymes (58) into HA and free paclitaxel, which has the ability to act on microtubules. Although it is entirely possible the HA-paclitaxel conjugate can act on the microtubules without being enzymatically cleaved.

The overarching goal of this work was to determine if our ultra-small nanoconjugate would have efficacy in a preclinical triple negative brain metastases of breast cancer model. In agreement with our previous reports (5) paclitaxel did not improve the median survival time (Control: 37 days; paclitaxel: 42 days p=0.4524). However, as shown in Fig. 7B HA-paclitaxel significantly improved the overall survival time from 37 days to 49 days (p=0.035). To best of our knowledge, this is the first report to show the *in vivo* efficacy of HA-paclitaxel bioconjugate in a preclinical model of brain metastases of breast cancer. It is of interest, that 24 hours after intracardiac injection of the Luc-2 transfected 231Br cells, most animals had luminescent signal only in the brain region, while a few animals had bioluminescent signal in the kidney, liver and bladder region. We speculate that the 231Br cells when injected, rapidly seed the brain (within 24 h) and most if not all remaining metastatic cells are cleared from the body.

The results presented in this manuscript suggest that low molecular weight HA could be effective in delivering drug to brain metastases of breast cancer. Further work should be completed to determine if this platform is effective in the delivering other chemotherapeutics or potentially combinatorial therapy. These data could be used in the development of other preclinical studies evaluating pharmacokinetics and toxicity.

Supplementary Material

Refer to Web version on PubMed Central for supplementary material.

Acknowledgements:

We acknowledge Dr. Liangxi Li in the Department of Pharmaceutical Sciences, Texas Tech University for helping synthesis of conjugates; Dr. M. Zeller in the Department of Chemistry, Youngstown University (Youngstown OH), for assisting with the NMR spectroscopy data.

Funding for this study was provided by the Department of Defense, Breast Cancer Research Program, grant W81 XWH-062-0033 (to P.S. Steeg, D. Palmieri, Q.R. Smith and P.R. Lockman).

References:

1. Palmieri D, Bronder JL, Herring JM, Yoneda T, Weil RJ, Stark AM, et al.Her-2 overexpression increases the metastatic outgrowth of breast cancer cells in the brain. Cancer Res. 2007;67:4190–8. [PubMed: 17483330]
2. Weil RJ, Palmieri DC, Bronder JL, Stark AM, Steeg PS. Breast cancer metastasis to the central nervous system. Am J Pathol. 2005;167:913–20. [PubMed: 16192626]

3. Lin NU, Bellon JR, Winer EP. CNS metastases in breast cancer. J Clin Oncol. 2004;22:3608–17. [PubMed: 15337811]
4. Peereboom DM. Chemotherapy in brain metastases. Neurosurgery. 2005;57:S54–65; discusssion S1–4. [PubMed: 16237290]
5. Lockman PR, Mittapalli RK, Taskar KS, Rudraraju V, Gril B, Bohn KA, et al.Heterogeneous blood-tumor barrier permeability determines drug efficacy in experimental brain metastases of breast cancer. Clin Cancer Res. 2010;16:5664–78. [PubMed: 20829328]
6. Deeken JF, Loscher W. The blood-brain barrier and cancer: transporters, treatment, and Trojan horses. Clin Cancer Res. 2007;13:1663–74. [PubMed: 17363519]
7. Smith QR. Brain perfusion systems for studies of drug uptake and metabolism in the central nervous system. Pharm Biotechnol. 1996;8:285–307. [PubMed: 8791815]
8. Pardridge WM. Blood-brain barrier delivery. Drug Discov Today. 2007;12:54–61. [PubMed: 17198973]
9. Kemper EM, van Zandbergen AE, Cleypool C, Mos HA, Boogerd W, Beijnen JH, et al.Increased penetration of paclitaxel into the brain by inhibition of P-Glycoprotein. Clin Cancer Res. 2003;9:2849–55. [PubMed: 12855665]
10. Sparreboom A, van Tellingen O, Nooijen WJ, Beijnen JH. Tissue distribution, metabolism and excretion of paclitaxel in mice. Anticancer Drugs. 1996;7:78–86. [PubMed: 8742102]
11. Jaracz S, Chen J, Kuznetsova LV, Ojima I. Recent advances in tumor-targeting anticancer drug conjugates. Bioorg Med Chem. 2005;13:5043–54. [PubMed: 15955702]
12. Ghosh SC, Neslihan Alpay S, Klostergaard J. CD44: a validated target for improved delivery of cancer therapeutics. Expert Opin Ther Targets. 2012;16:635–50. [PubMed: 22621669]
13. Leonelli F, La Bella A, Migneco LM, Bettolo RM. Design, synthesis and applications of hyaluronic acid-paclitaxel bioconjugates. Molecules. 2008;13:360–78. [PubMed: 18305424]
14. Singh SK, Clarke ID, Hide T, Dirks PB. Cancer stem cells in nervous system tumors. Oncogene. 2004;23:7267–73. [PubMed: 15378086]
15. Jordan CT, Guzman ML. Mechanisms controlling pathogenesis and survival of leukemic stem cells. Oncogene. 2004;23:7178–87. [PubMed: 15378078]
16. Al-Hajj M, Wicha MS, Benito-Hernandez A, Morrison SJ, Clarke MF. Prospective identification of tumorigenic breast cancer cells. Proc Natl Acad Sci U S A. 2003;100:3983–8. [PubMed: 12629218]
17. Al-Hajj M, Clarke MF. Self-renewal and solid tumor stem cells. Oncogene. 2004;23:7274–82. [PubMed: 15378087]
18. Reya T, Morrison SJ, Clarke MF, Weissman IL. Stem cells, cancer, and cancer stem cells. Nature. 2001;414:105–11. [PubMed: 11689955]
19. Vercruysse KP, Prestwich GD. Hyaluronate derivatives in drug delivery. Crit Rev Ther Drug Carrier Syst. 1998;15:513–55. [PubMed: 9822869]
20. Rosato A, Banzato A, De Luca G, Renier D, Bettella F, Pagano C, et al.HYTAD1-p20: a new paclitaxel-hyaluronic acid hydrosoluble bioconjugate for treatment of superficial bladder cancer. Urol Oncol. 2006;24:207–15. [PubMed: 16678050]
21. Banzato A, Bobisse S, Rondina M, Renier D, Bettella F, Esposito G, et al.A paclitaxel-hyaluronan bioconjugate targeting ovarian cancer affords a potent in vivo therapeutic activity. Clin Cancer Res. 2008;14:3598–606. [PubMed: 18519794]
22. Yoon HY, Koo H, Choi KY, Chan Kwon I, Choi K, Park JH, et al.Photo-crosslinked hyaluronic acid nanoparticles with improved stability for in vivo tumor-targeted drug delivery. Biomaterials. 2013.
23. Yang XY, Li YX, Li M, Zhang L, Feng LX, Zhang N. Hyaluronic acid-coated nanostructured lipid carriers for targeting paclitaxel to cancer. Cancer Lett. 2012.
24. Das M, Singh RP, Datir SR, Jain S. Surface chemistry dependent “switch” regulates the trafficking and therapeutic performance of drug-loaded carbon nanotubes. Bioconjug Chem. 2013;24:626–39. [PubMed: 23517108]

25. Jin YJ, Termsarasab U, Ko SH, Shim JS, Chong S, Chung SJ, et al.Hyaluronic acid derivative-based self-assembled nanoparticles for the treatment of melanoma. Pharm Res. 2012;29:3443–54. [PubMed: 22886625]
26. Fairchild CR, Moscow JA, O'Brien EE, Cowan KH. Multidrug resistance in cells transfected with human genes encoding a variant P-glycoprotein and glutathione S-transferase-pi. Mol Pharmacol. 1990;37:801–9. [PubMed: 1972772]
27. Rao PS, Mallya KB, Srivenugopal KS, Balaji KC, Rao US. RNF2 interacts with the linker region of the human P-glycoprotein. Int J Oncol. 2006;29:1413–9. [PubMed: 17088979]
28. Lee H, Lee K, Park TG. Hyaluronic acid-paclitaxel conjugate micelles: synthesis, characterization, and antitumor activity. Bioconjug Chem. 2008;19:1319–25. [PubMed: 18481885]
29. Cai S, Xie Y, Bagby TR, Cohen MS, Forrest ML. Intralymphatic chemotherapy using a hyaluronan-cisplatin conjugate. J Surg Res. 2008;147:247–52. [PubMed: 18498877]
30. Yoneda T, Williams PJ, Hiraga T, Niewolna M, Nishimura R. A bone-seeking clone exhibits different biological properties from the MDA-MB-231 parental human breast cancer cells and a brain-seeking clone in vivo and in vitro. J Bone Miner Res. 2001;16:1486–95. [PubMed: 11499871]
31. Wang LH, Rothberg KG, Anderson RG. Mis-assembly of clathrin lattices on endosomes reveals a regulatory switch for coated pit formation. J Cell Biol. 1993;123:1107–17. [PubMed: 8245121]
32. Brown DA. Lipid rafts, detergent-resistant membranes, and raft targeting signals. Physiology (Bethesda). 2006;21:430–9. [PubMed: 17119156]
33. Lee JL, Wang MJ, Sudhir PR, Chen JY. CD44 engagement promotes matrix-derived survival through the CD44-SRC-integrin axis in lipid rafts. Mol Cell Biol. 2008;28:5710–23. [PubMed: 18644869]
34. Manunta M, Tan PH, Sagoo P, Kashefi K, George AJ. Gene delivery by dendrimers operates via a cholesterol dependent pathway. Nucleic Acids Res. 2004;32:2730–9. [PubMed: 15148360]
35. Rowinsky EK, Donehower RC, Jones RJ, Tucker RW. Microtubule changes and cytotoxicity in leukemic cell lines treated with taxol. Cancer Res. 1988;48:4093–100. [PubMed: 2898289]
36. Schiff PB, Fant J, Horwitz SB. Promotion of microtubule assembly in vitro by taxol. Nature. 1979;277:665–7. [PubMed: 423966]
37. Anders C, Carey LA. Understanding and treating triple-negative breast cancer. Oncology (Williston Park). 2008;22:1233–9; discussion 9–40, 43. [PubMed: 18980022]
38. Li H, Liu J, Hofmann M, Hamou MF, de Tribolet N. Differential CD44 expression patterns in primary brain tumours and brain metastases. Br J Cancer. 1995;72:160–3. [PubMed: 7541233]
39. Ranuncolo SM, Ladeda V, Specterman S, Varela M, Lastiri J, Morandi A, et al.CD44 expression in human gliomas. J Surg Oncol. 2002;79:30–5; discussion 5–6. [PubMed: 11754374]
40. Peer D, Margalit R. Tumor-targeted hyaluronan nanoliposomes increase the antitumor activity of liposomal Doxorubicin in syngeneic and human xenograft mouse tumor models. Neoplasia. 2004;6:343–53. [PubMed: 15256056]
41. Auzenne E, Ghosh SC, Khodadadian M, Rivera B, Farquhar D, Price RE, et al.Hyaluronic acid-paclitaxel: antitumor efficacy against CD44(+) human ovarian carcinoma xenografts. Neoplasia. 2007;9:479–86. [PubMed: 17603630]
42. Luo Y, Ziebell MR, Prestwich GD. A hyaluronic acid-taxol antitumor bioconjugate targeted to cancer cells. Biomacromolecules. 2000;1:208–18. [PubMed: 11710102]
43. Luo Y, Prestwich GD. Synthesis and selective cytotoxicity of a hyaluronic acid-antitumor bioconjugate. Bioconjug Chem. 1999;10:755–63. [PubMed: 10502340]
44. Lesley J, Hascall VC, Tammi M, Hyman R. Hyaluronan binding by cell surface CD44. J Biol Chem. 2000;275:26967–75. [PubMed: 10871609]
45. Geney R, Ungureanu M, Li D, Ojima I. Overcoming multidrug resistance in taxane chemotherapy. Clin Chem Lab Med. 2002;40:918–25. [PubMed: 12435109]
46. Kemper EM, Boogerd W, Thuis I, Beijnen JH, van Tellingen O. Modulation of the blood-brain barrier in oncology: therapeutic opportunities for the treatment of brain tumours?Cancer Treat Rev. 2004;30:415–23. [PubMed: 15245774]

47. Rice A, Liu Y, Michaelis ML, Himes RH, Georg GI, Audus KL. Chemical modification of paclitaxel (Taxol) reduces P-glycoprotein interactions and increases permeation across the blood-brain barrier in vitro and in situ. J Med Chem. 2005;48:832–8. [PubMed: 15689167]

48. Nikanjam M, Gibbs AR, Hunt CA, Budinger TF, Forte TM. Synthetic nano-LDL with paclitaxel oleate as a targeted drug delivery vehicle for glioblastoma multiforme. J Control Release. 2007;124:163–71. [PubMed: 17964677]

49. Blanc E, Bonnafous C, Merida P, Cisternino S, Clair P, Scherrmann JM, et al.Peptide-vector strategy bypasses P-glycoprotein efflux, and enhances brain transport and solubility of paclitaxel. Anticancer Drugs. 2004;15:947–54. [PubMed: 15514563]

50. Demeule M, Regina A, Che C, Poirier J, Nguyen T, Gabathuler R, et al.Identification and Design of New Peptides as a Drug Delivery System for the Brain. J Pharmacol Exp Ther. 2007.

51. Thomas FC, Taskar K, Rudraraju V, Goda S, Thorsheim HR, Gaasch JA, et al.Uptake of ANG1005, A Novel Paclitaxel Derivative, Through the Blood-Brain Barrier into Brain and Experimental Brain Metastases of Breast Cancer. Pharm Res. 2009.

52. Regina A, Demeule M, Che C, Lavallee I, Poirier J, Gabathuler R, et al.Antitumour activity of ANG1005, a conjugate between paclitaxel and the new brain delivery vector Angiopep-2. Br J Pharmacol. 2008.

53. Rousselle C, Clair P, Lefauconnier JM, Kaczorek M, Scherrmann JM, Temsamani J. New advances in the transport of doxorubicin through the blood-brain barrier by a peptide vector-mediated strategy. Molecular pharmacology. 2000;57:679–86. [PubMed: 10727512]

54. Che C, Yang G, Thiot C, Lacoste MC, Currie JC, Demeule M, et al.New Angiopep-modified doxorubicin (ANG1007) and etoposide (ANG1009) chemotherapeutics with increased brain penetration. J Med Chem. 2010;53:2814–24. [PubMed: 20210346]

55. Regina A, Demeule M, Che C, Lavallee I, Poirier J, Gabathuler R, et al.Antitumour activity of ANG1005, a conjugate between paclitaxel and the new brain delivery vector Angiopep-2. Br J Pharmacol. 2008;155:185–97. [PubMed: 18574456]

56. Mazel M, Clair P, Rousselle C, Vidal P, Scherrmann JM, Mathieu D, et al.Doxorubicin-peptide conjugates overcome multidrug resistance. Anticancer Drugs. 2001;12:107–16. [PubMed: 11261883]

57. Crown J, O'Leary M. The taxanes: an update. Lancet. 2000;355:1176–8. [PubMed: 10791395]

58. Liu D, Pearlman E, Diaconu E, Guo K, Mori H, Haqqi T, et al.Expression of hyaluronidase by tumor cells induces angiogenesis in vivo. Proc Natl Acad Sci U S A. 1996;93:7832–7. [PubMed: 8755562]

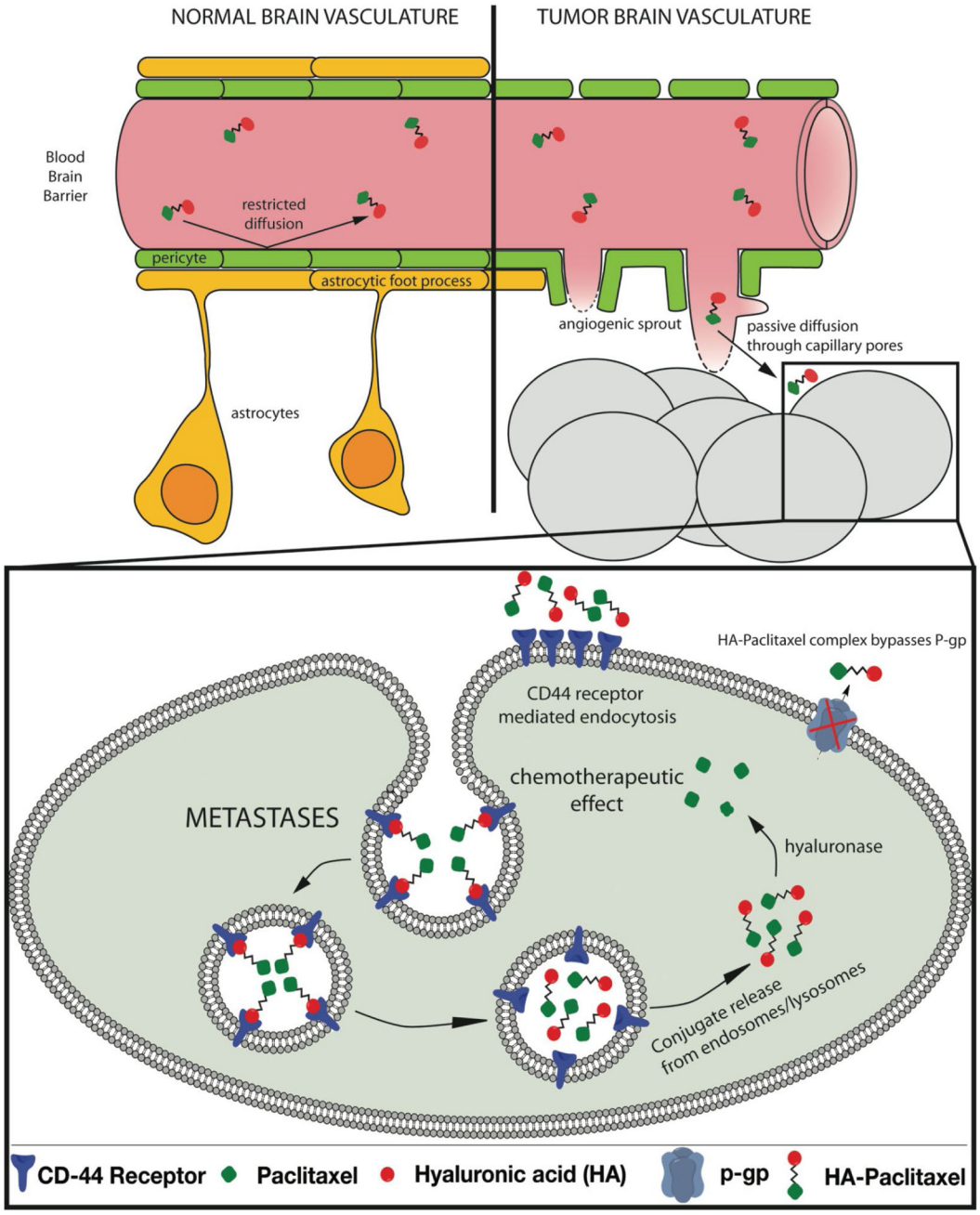

Figure 1:

Schematic diagram of HA-paclitaxel nanoconjugates hypothetical mechanism of action using CD44 receptor-mediated endocytosis.

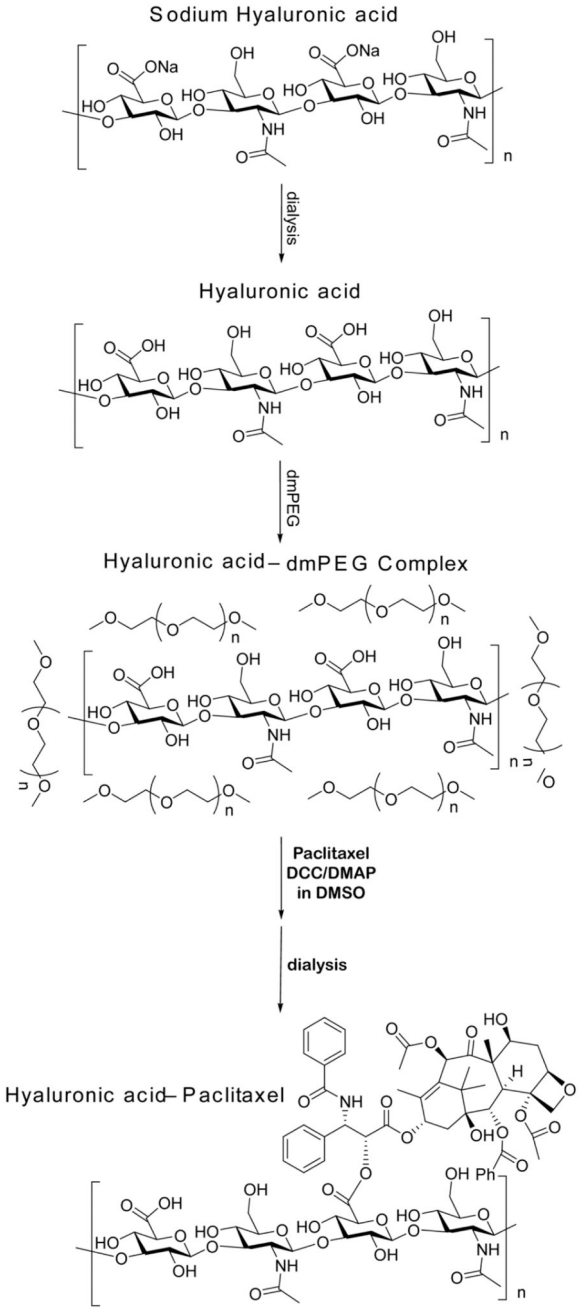

Figure 2:

Chemical structure and synthetic scheme for HA-Paclitaxel. Briefly, in the first step the sodium hyaluronic acid was desalted using dialysis against water. In the second step, a nanocomplex was formed between HA and dmPEG. In the last step, the HA-dmPEG complex was conjugated to paclitaxel using a carbodiimide reaction.

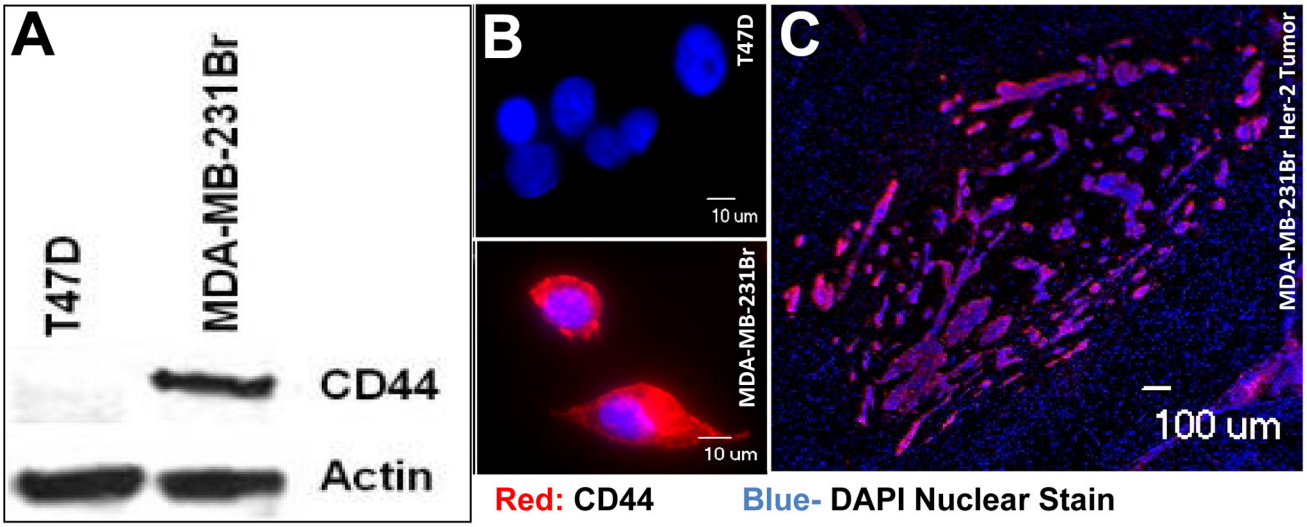

Figure 3:

CD44 is expressed on the cell surface in 231Br cells. Relative expression (**A**) of CD44 in 231Br cells compared to T47D cells which do not express the receptor. (**B**) Immunocytochemistry suggests membrane distribution of CD44. **C)** Representative image demonstrating that a high degree of CD44 expression is retained in 231Br brain metastases *in vivo*.

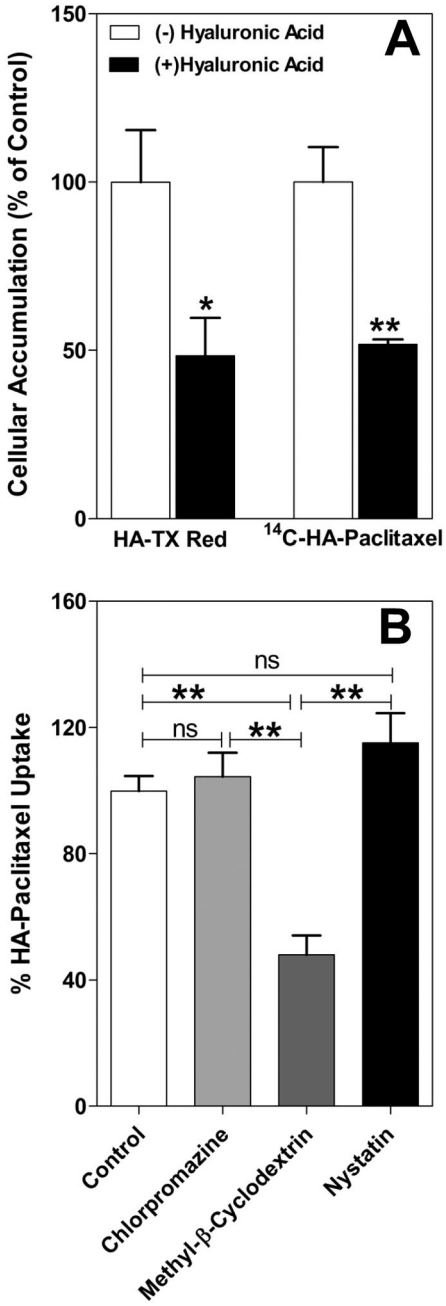

Figure 4:

HA-TX Red and ^{14}C-HA-paclitaxel accumulate in 231Br cells via CD44 receptormediated endocytocis. (**A)** The *in vitro* uptake of HA-TX Red and ^{14}C-HA-Paclitaxel was reduced ~50% by the presence of free 1600kDa HA (0.625 μM) which effectively competes for CD44 receptor-mediated endocytocis. **(B)** Pharmacological inhibition of clathrin mediated endocytosis by incubation with chlorpromazine hydrochloride (10 μg/mL) for 30 minutes and caveolae mediated endocytosis uptake by 25 μg/mL nystatin did not inhibit HA-paclitaxel uptake into 231Br cells ($p>0.05$). However, inhibition of the lipid raft endocytosis pathway with 5 mM methyl-β-cyclodextrin significantly reduced the uptake of ^{14}C-HA-

paclitaxel into 231Br cells as compared to control ($p<0.01$). These data suggest the conjugate is actively taken into 231Br cells via CD44 mediated endocytocis. Data represent Mean ± SEM; n=6. A *, **, and ***, represent significant p values of $p< 0.05$, 0.01, and 0,001 respectively.

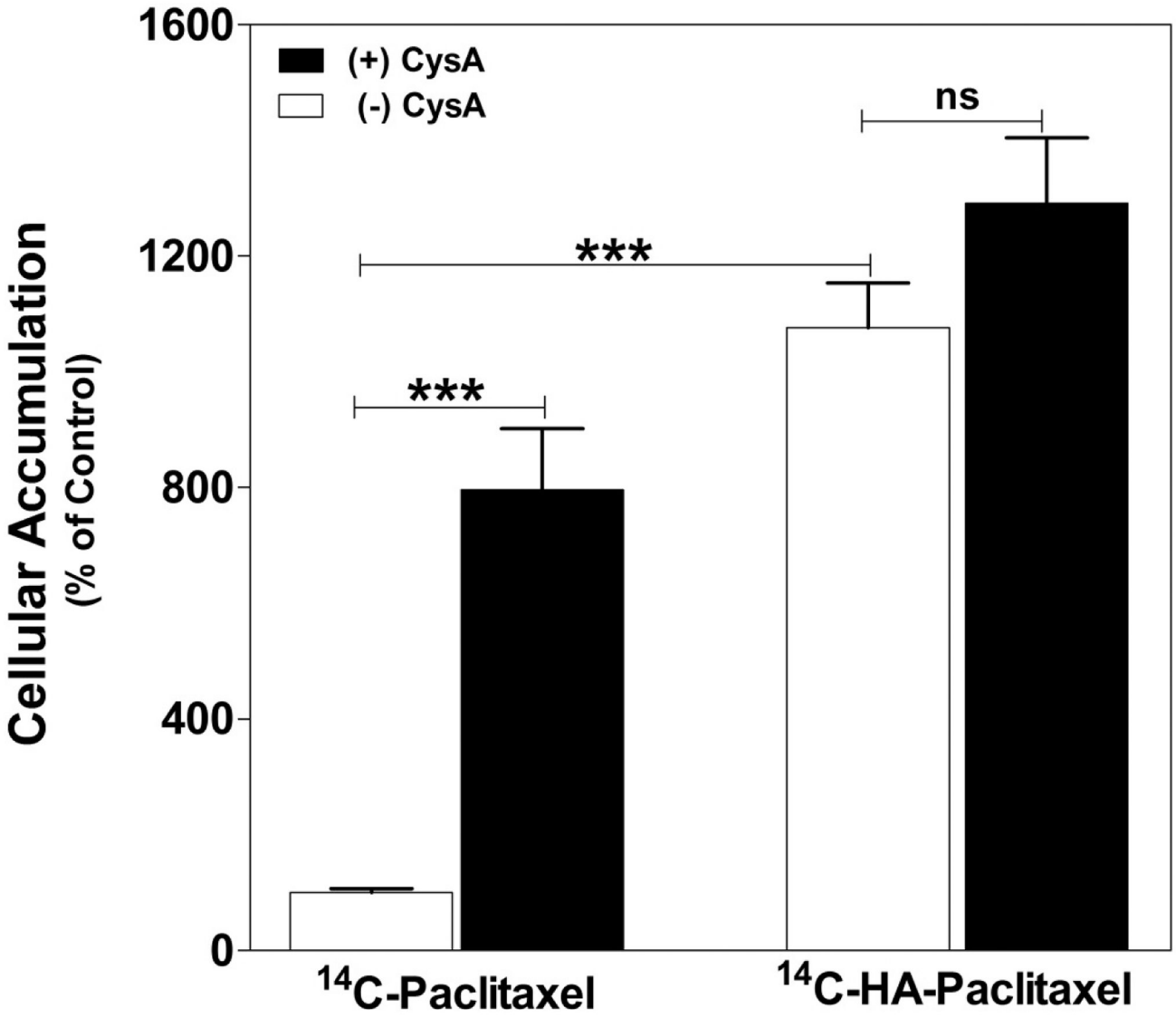

Figure 5:

HA-paclitaxel bypasses P-gp mediated efflux of paclitaxel. In control experiments, an ~8 fold increase in ^{14}C-paclitaxel cellular accumulation was observed in presence of the P-gp inhibitor, cyclosporine A (10 μM) in 30 min *in vitro* uptake experiments (left bars). In contrast cellular uptake of ^{14}C-HA-paclitaxel was ~11 fold greater than control ^{14}C-paclitaxel uptake and was not reduced by the presence of 10 μM cyclosporine A (right bars). Data represent Mean ± SEM; n=6. A *, **, and ***, represent significant p values of p< 0.05, 0.01, and 0.001 respectively (ANOVA).

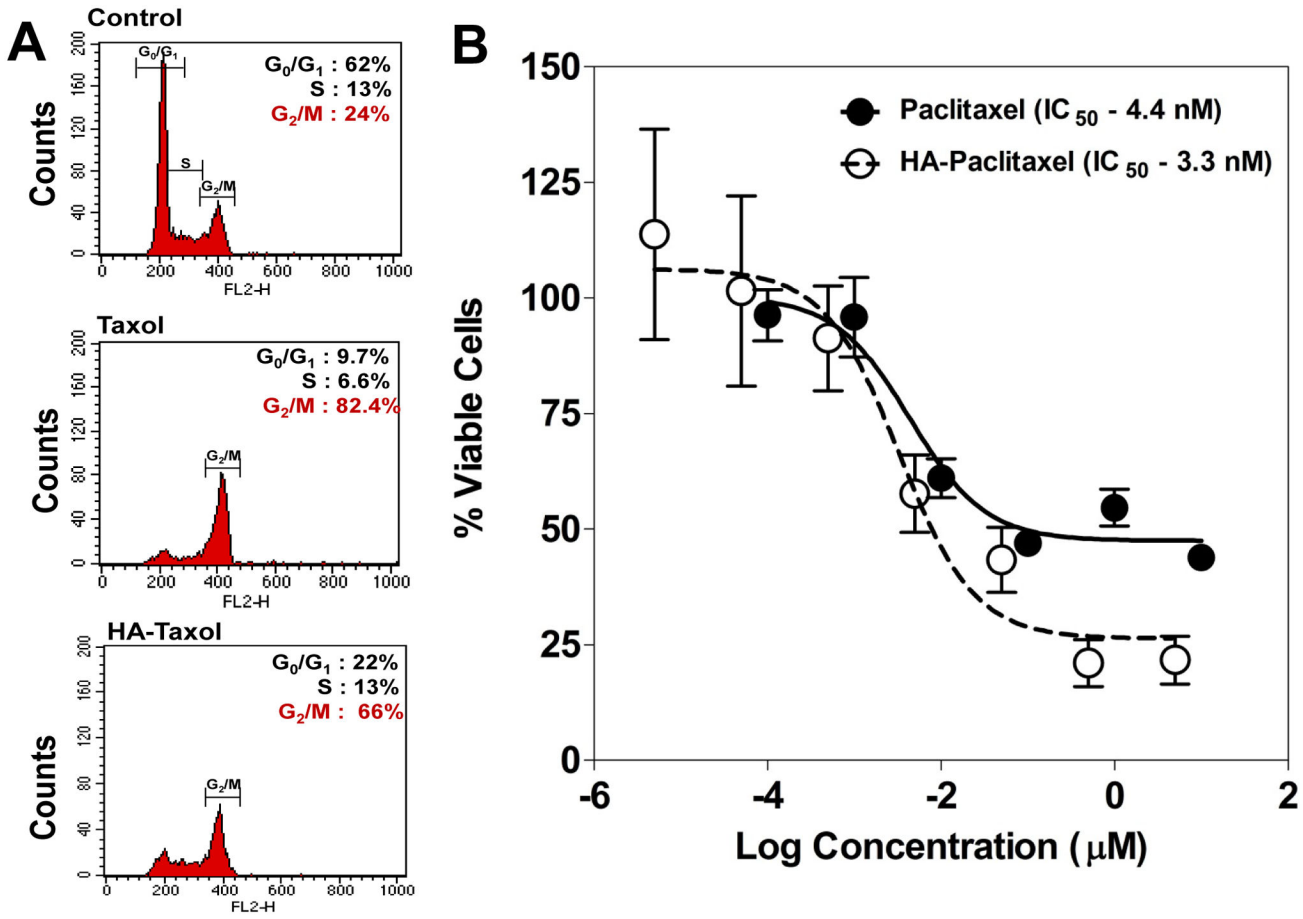

Figure 6:

Paclitaxel and HA-paclitaxel exert similar cytotoxicity profiles. (**A**) Representative cell cycle analysis graphs of control, paclitaxel (100 nM) treated and HA-paclitaxel (100 nM paclitaxel equivalent) treated 231Br cells. Both paclitaxel and HA-paclitaxel caused significant (n=3, $p<0.05$) cell cycle arrest at the G_2/M phase (70 ± 12% and 56 ± 10% of cells respectively) as compared to control (17 ± 7%). (**B**) *In vitro* cytotoxicity of HA-paclitaxel and paclitaxel in 231Br cells. 231Br cell cultures were incubated with paclitaxel or HA-paclitaxel for 48 hrs at concentrations ranging from 0.1 nM to 10 μM. The number of viable cells at 48 hrs was determined using MTT assay. Data represent Mean ± SEM; n=6 for all points. IC_{50} was calculated using log dose response curve ($P>0.05$).

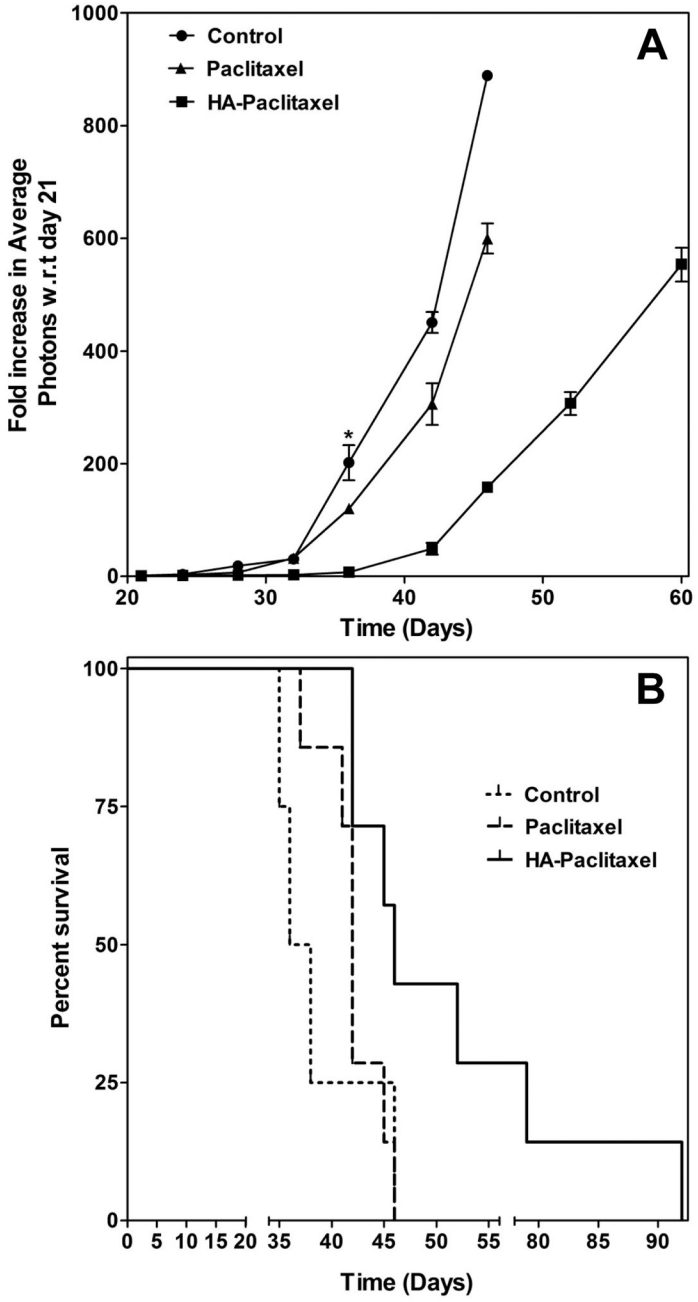

Figure 7:

HA-paclitaxel formulation prolongs overall survival. (**A**) Significant decrease in metastatic lesion burden as measured by BLI was observed in the HA-paclitaxel treated groups compared with control and paclitaxel ($p<0.05$). (**B**) Median survival was prolonged as determined by the log rank test in the HA-paclitaxel group compared to control ($p = 0.35$) and the paclitaxel treated group ($p = 0.28$); n=7 for all groups.